Monodisperse Twin Liquid Crystalline Macromolecules. 2. Molecular Dynamics

C. W. Chu, L. Charles Dickinson, and James C. W. Chien*

Department of Polymer Science and Engineering and Department of Chemistry, University of Massachusetts, Amherst, Massachusetts 01003

Received December 19, 1990; Revised Manuscript Received August 27, 1991

ABSTRACT: Solid-state ^{13}C NMR studies have been performed on monodisperse twin liquid crystalline macromolecules (TLCM) of the M–S–M type where M is a mesogen $BuO(C_6H_4COO-)_x$, ($x = 2$ or 3 for TLCM-II or TLCM-III), and S is monodisperse poly(tetrahydrofuran) (PTHF) or poly(propylene glycol) (PPG) having molecular weights of 625–2000. TLCM-IIs exhibit nematic texture while TLCM-IIIs display a smectic phase. Cross polarization and direct polarization modes were used to obtain NMR spectra of the TLCMs in crystalline, mesophasic, and isotropic states. Dipolar dephasing was used to assist the assignment of the resonances of carbons with or without hydrogens. Measurement of the change of magnetization intensity with spin-lock contact time affords the determination of cross polarization time and spin–lattice relaxation time in the rotating frame. In the crystalline states of TLCMs, the M termini including the butoxy groups are rigid whereas the central S segments are free to rotate. The motional freedom of the macromolecules in the mesophase is dependent on the temperature. Thus, the butoxy groups in the TLCM-IIs are rigid in the nematic state at 45 °C, whereas the butoxy groups in the TLCM-IIIs are freely rotating in the smectic state at 90 °C. TLCMs with PTHF as S are microphase separated in the mesophase; the TLCMs with PPG as S are not phase separated. Phase separation in the former seems to persist even above the isotropization temperature.

Introduction

Twin liquid crystalline compounds having two mesogenic units (M) linked by $(CH_2)_n$ ($n = 2$–12) have been described.[1-5] The possibility that higher MW materials with similar structural arrangements may exhibit mesophases was investigated by Lenz and co-workers.[6] They end capped α,ω-dihydroxypoly(ethylene oxide) ($\bar{M}_n = 1750$) (S) with $HOOC-C_6H_4-CO_2-C_6H_4CO_2-$ and its benzyl ester precursor. These polymers exhibited weak liquid crystalline textures over only a few degrees in temperature. Some of the reasons for the poor liquid crystallinity are low aspect ratio of the mesogen, flexibility of the spacer, and the molecular weight polydispersity of S.

We have reported the synthesis of monodisperse liquid crystalline macromolecules (TLCM) of the M–S–M type,[7] where M is an aromatic diester and S is poly(tetrahydrofuran) (PTHF). Two structural considerations, believed to be important in fostering mesophase formation, are the monodispersity of S and the length of the terminal alkyl group. In the phase-separated mesostate above T_{KM} (crystal to mesophase transition temperature), the TLCM displayed high elasticity to small amplitude deformation and shear thinning at large deformation.[8] The mesogenic domains function as physical cross-links both in the mesophase and above T_{MI} (mesophase to isotropic transition temperature). Only at a higher coexistence temperature[9] (T_{IC}), the TLCM becomes single phased and behaves like a common low molecular weight homopolymer.

We have now made further investigation of TLCMs varying the sizes and nature of both M and S with the aim to reveal structure–property relationships. The synthesis of these TLCMs and the properties associated with liquid crystallinity were described in part 1.[10] The synthesis involved preparative thin-layer chromatography which produces milligram quantities of TLCM. By repeating the synthesis many times, we accumulated sufficient amounts of several TLCMs for studies by rheological techniques and solid-state NMR. The NMR results are presented in this paper.

Experimental Section

Materials. The monodispersed TLCMs were synthesized in our laboratory by R. Zhou.[10] The sample designations, structures, and thermotropic transition properties are summarized in Table I.

NMR. The ^{13}C solid-state NMR measurements were performed on a Bruker 200 AF spectrometer with IBM Instruments Solid Accessory and a Doty Scientific cross polarization/magic angle spinning (CP/MAS) probe. The spectrometer was operated at a carbon frequency of 50.3 MHz. Matched spin-lock cross polarization (CP) transfer employed H_1 (spin-lock field) with a 5-μs π/2 pulse, a variable contact time (τ), and a 3-s recycle time. In the dipolar dephasing sequence, a delay period of 10–50 μs was inserted between the end of the cross polarization sequence and the onset of high-power proton decoupling and data acquisition. Samples were packed into a sapphire rotor which was fitted with axial-screw Kel-F end caps to avoid slippage during spinning. The spinning speed was from 3 to 4 kHz using compressed air or N_2 gas. For variable-temperature measurement, a Bruker VT B-1000 temperature controller was used to heat the spinning gas and control the temperature to ±2 °C. Solution ^{13}C NMR was performed on a Varian XL-200 spectrometer. Direct polarization (DP) spectra were obtained using a simple π/2 pulse.

Results and Discussion

TLCM-II–PTHF(650). This polymer has $T_{KM} = 26$ °C and $T_{MI} = 48$ °C. Its structure and the ^{13}C assignments are as follows.

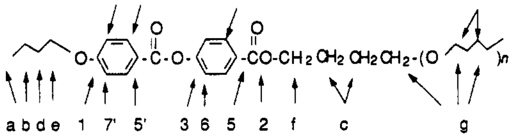

(1)

The chemical shift values for all the carbons are given in Table II.

The spectrum of the crystalline state was obtained using the CP/MAS mode at 0 °C; the aromatic region is shown in Figure 1a. The assignment of carbon 5 and 5′ to the nonprotonated aromatic carbons was based on the results

0024-9297/92/2225-0201$03.00/0

Table I
Monodispersed Twin Liquid Crystalline Macromolecules

sample notation	M	S (MW)	transitions,[a] °C
TLCM-II–PTHF(650)	$BuOC_6H_4CO_2C_6H_4CO_2$–(II)	THF[b] (650)	K26N48I
TLCM-II–PPG(625)	II	PPG[c] (625)	K32N58I
TLCM-II–PPG(800)	II	PPG (800)	K20N53I
TLCM-III–PPG(725)	$BuOC_6H_4CO_2C_6H_4CO_2C_6H_4CO_2$–(III)	PPG (725)	K78S110I
TLCM-III–PTHF(650)	III	PTHF (650)	$K_182K_2110S165I$
TLCM-III–PTHF(2000)	III	PTHF (2000)	K78S103I

[a] K = crystalline, N = nematic, S = smectic, and I = isotropic. [b] Poly(tetrahydrofuran). [c] Poly(propylene glycol).

Table II
Chemical Shift Values for TLCM-II–PTHF

	chemical shift, ppm			
carbon type	solid, isotropic	soln	solid, crystalline	calcd[b]
aromatic				
1	165.0	164.3	164.0	165.0
2	163.5	163.7	162.6	
3	154.7	154.8	154.4	155.0
4	132.0	132.3	131.0	131.0
4′	130.6	131.0	130.5	128.0
5	127.6	127.8	127.8	127.0
5′	127.6	121.0	122.0	123.0
6	121.5	121.8	122.3	121.6
7	114.3	114.3	116.3	114.1
7′	114.3	114.3	109.1	114.1
aliphatic				
a	13.4	14.0	13.9	
b	18.9	19.2	*c*	
c	26.3	26.6	26.6	
d	30.9	31.2	*c*	
e	64.6	64.9	*c*	
f	67.8	68.1	*c*	
g	70.2	70.8	70.4	

[a] DP. [b] Calculated. [c] Overlapped with the PTHF peaks.

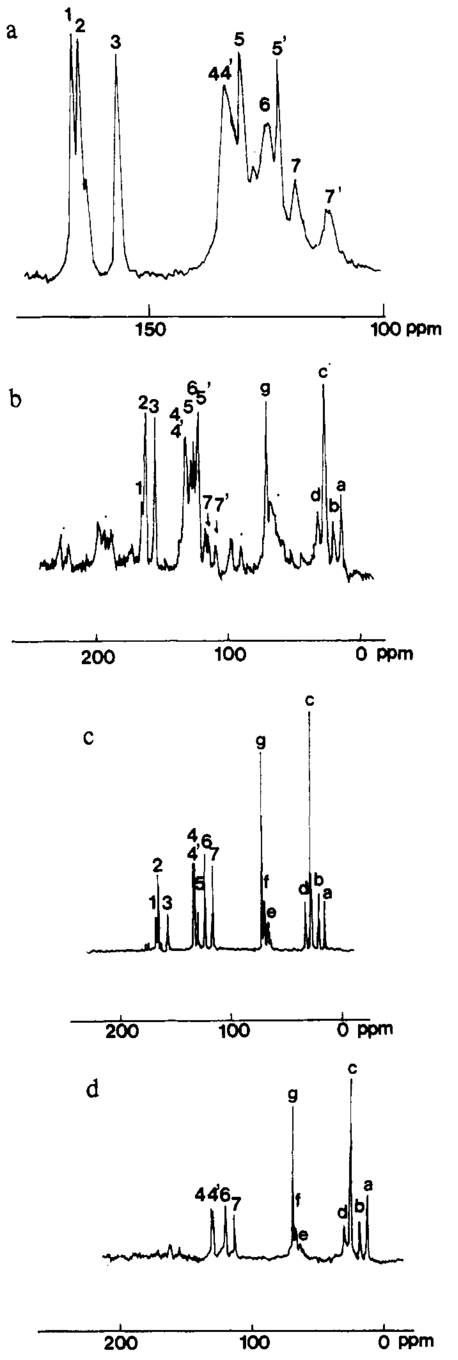

Figure 1. ^{13}C NMR spectra of TLCM-II–PTHF(650): (a) crystalline state at 0 °C (CP); (b) nematic state at 40 °C (CP); (c) isotropic state at 60 °C (DP); (d) isotropic state at 60 °C (CP).

of dipolar dephasing experiments. During the delay period, those carbons with strong carbon–proton coupling were significantly relaxed, thus allowing preferential detection of those carbons with weak carbon–proton coupling.[11] Peaks 5 (127 ppm) and 5′ (120 ppm) remained intense after a delay of 50 μs so they were judged to be unprotonated carbons. The carbons 7 and 7′ ortho to the oxygen bonded to the phenyl ring have different chemical shifts in the solid state. These two peaks become a 114.4 ppm singlet in the melt (vide infra). The splitting could be caused by the fixed orientation of the butoxy group with respect to the benzene ring. Consequently, these carbons bear different spatial separation from the methylene carbon (C_e). This nonequivalence has also been observed in dimethoxybenzene,[12] *p*-alkoxybenzoic acid,[13] 4′-cyanophenyl 4-(amyloxy)benzoate,[14] and bis(4-butoxy-*p*-phenyl) terephthalate.[15] The resonance of C6 is broad, approximately 0.5 ppm in width. Another explanation is a libration of the aromatic ring about the ester linkage[15] which could affect line width. The broad peak between 130 and 132 ppm is assigned to the partially overlapping C4 and C4′ peaks.

The CP/MAS spectrum (Figure 1b) recorded at 40 °C for the mesophase showed clear nonequivalencies for C7 and C7′. Therefore, the mesogens are substantially restricted in motion. Aside from this similarity between the crystalline and the mesophasic states, there are differences in their NMR spectra. The protonated aromatic carbon resonances at 40 °C are about 3 times broader than at 0 °C (400 Hz vs 125 Hz). This line broadening was not observed for the nonprotonated aromatic carbons. The major contribution for line broadening[17] is either from the modulation of the chemical shift anisotropy by molecular motion at frequencies close to the sample spinning frequency or from the modulation of the ^{13}C–^{1}H dipolar coupling at frequencies close to the decoupler field. The chemical shift anisotropy of the carbon of the protonated and unprotonated aromatic carbons are similar. The fact that only the protonated aromatic carbons are broadened suggests that the modulation of the ^{13}C–^{1}H interaction is the dominant mechanism. In contrast to the protonated aromatic carbons, the line width of the methylene carbons in S decreases from 200 Hz in the crystalline state to 50 Hz in the mesophase. Therefore there is motional averaging of the carbon–proton dipolar interactions in the liquid crystalline state for the PTHF segment.

The spectra of the isotropic state, obtained at 60 °C by DP and CP/MAS, are given in Figure 1c,d, respectively. Comparison with Figure 1 reveals that the aromatic carbons resonate at slightly higher fields (0.5–1 ppm) in the crystalline state. This increase in shielding could arise from a closer stacking of the mesogens in the solid state or from restrictions in conformational arranging in the crystalline state. The DP spectrum is identical to the solution spectrum. There is only a single peak at 114 ppm in the 116–110 ppm region. This implies that the butoxy group is freely rotating about the O–C_1 axis, making C7 and C7′ equivalent. The main difference between the CP and DP spectra is that the nonprotonated aromatic carbons were not detected by the CP mode even at long contact times. It is commonly assumed that cross polarization is ineffective for molecules undergoing rapid and isotropic tumbling because the dipolar coupling tensor has zero trace. The consequent reduction of both the second moment, $\langle M^2{}_{CH} \rangle$, and cross polarization efficiency can be calculated for various molecular reorientational motions. For instance, a rotation about an axis inclined at a 60° angle to the internuclear C–H vector can reduce the efficiency of cross polarization by a factor of 64. For a 180° jump between two sites such that the internuclear vector reorients through 120°, the $\langle M^2{}_{CH} \rangle$ is reduced by a factor of 2.3. The poor observability for nonprotonated aromatic carbons is undoubtedly due to free rotation of the butoxy group which renders CP ineffective.

TLCM-II–PPG. The carbon type assignments for the TLCM-II–PPGs are as follows.

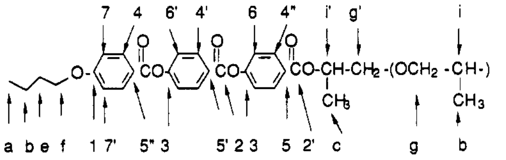

(2)

Their chemical shift values are given in Table III. The C7 and C7′ are nonequivalent for TLCM-II, with either 625 or 800 molecular weight PPG, in the CP/MAS spectrum for the crystalline state at 19 °C (Figure 2a).

The CP/MAS spectra for the mesophase obtained at 45 °C (Figure 2b) contained only the methyl carbon resonance of the PPG. No aromatic carbon resonances were observable, suggesting that the second moment of DD interactions between carbon and proton in the aromatic ring is dramatically reduced by rapid motion in the nematic phase, rendering magnetization transfer ineffective. Therefore, there is more freedom for motion in the TLCM with PPG as the spacer than those with PTHF for S.

Smectic TLCM. The CP ^{13}C NMR spectrum (aromatic region) of crystalline TLCM-III–PPG(725) obtained at room temperature is shown in Figure 3a; the peak assignments are listed in Table III. The C7 and C7′ resonances are clearly resolved at 116.6 and 108.4 ppm, respectively, which are at the same position as in the TLCM-II–PTHF(650) (vide supra). The line widths of aromatic peaks are only 1 ppm (50 Hz) which suggests that the chemical shift anisotropies of aromatic carbons having similar chemical environments were averaged by magic angle spinning.

Table III
Chemical Shift Values for TLCM with PPG Spacers

carbon type	chemical shifts, ppm 25 °C (crystalline)	90 °C (smectic)	120 °C (isotropic)
1	163.7	nd	nd[a]
2	162.7	162.4	162.6
2′	161.4	162.4	162.6
3	154.4	154.8	154.9
4	132.9	131.5	131.0
4′	131.7	131.5	131.0
4″	130.4	131.5	131.0
5	128	nd	nd
5′	125.5	nd	nd
5″	122	nd	nd
6	123.6	123.0	122.9
6′	122.8	123.0	122.9
7	116.6	114.6	114.6
7′	108.5	114.6	114.6
aliphatic			
a	14.2	13.8	13.6
b	17.9	17.4	17.0
c	oe	18.9	18.6
d	oe	nr	nr[c]
e	31.8	31.5	31.4
f	67.4	68.2	68.0
g′	oe	70	70.2
i′	oe	71.4	71.0
g	73.6	73.4	73.2
i	75.6	75.2	75.3

[a] nd, not detected by both CP and DP. [b] Overlap with offer carbons. [c] Not resolved.

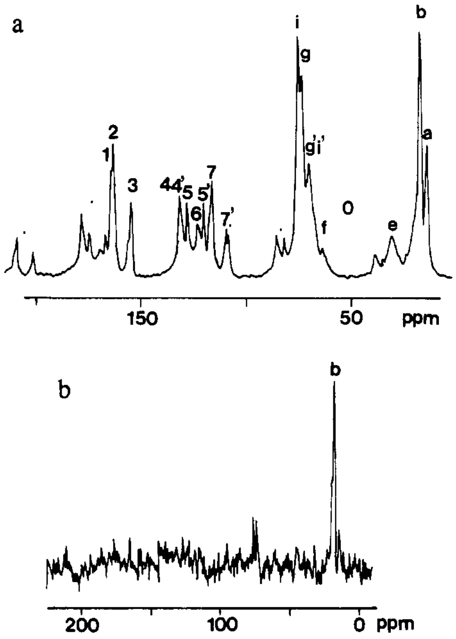

Figure 2. CP ^{13}C NMR spectrum of TLCM-II–PPG(625): (a) in the crystalline state at 18 °C; (b) in the nematic phase at 45 °C.

The protonated and nonprotonated aromatic carbons are differentiated by dipolar dephasing as above. Only the 128, 125.7, and 122 ppm peaks remained in this spectral region after a 50-μs delay. All the aromatic carbon resonances were resolved. The direct polarization spectra of TLCM-III–PPG(725) in the solid state contains only weak aromatic peaks because some of the carbons have long spin–lattice relaxation time ($T_1{}^C$). This implies that the frequency of motion for the C–H vector is much slower than 50 MHz (the frequency of the laboratory frame) and makes little contribution to the relaxation of carbon nuclei.

Figure 3b is the DP spectrum for the smectic phase obtained at 10 °C above the T_{KM} of TLCM-III–PPG(725). Essentially the same spectrum was obtained with the CP mode using long contact time. The interesting unexpected observation is that there is only a single peak at 115.5 ppm for both C7 carbons, whereas C7 and C7′ have different chemical shifts in the mesophases of TLCM-II–PPG(625)

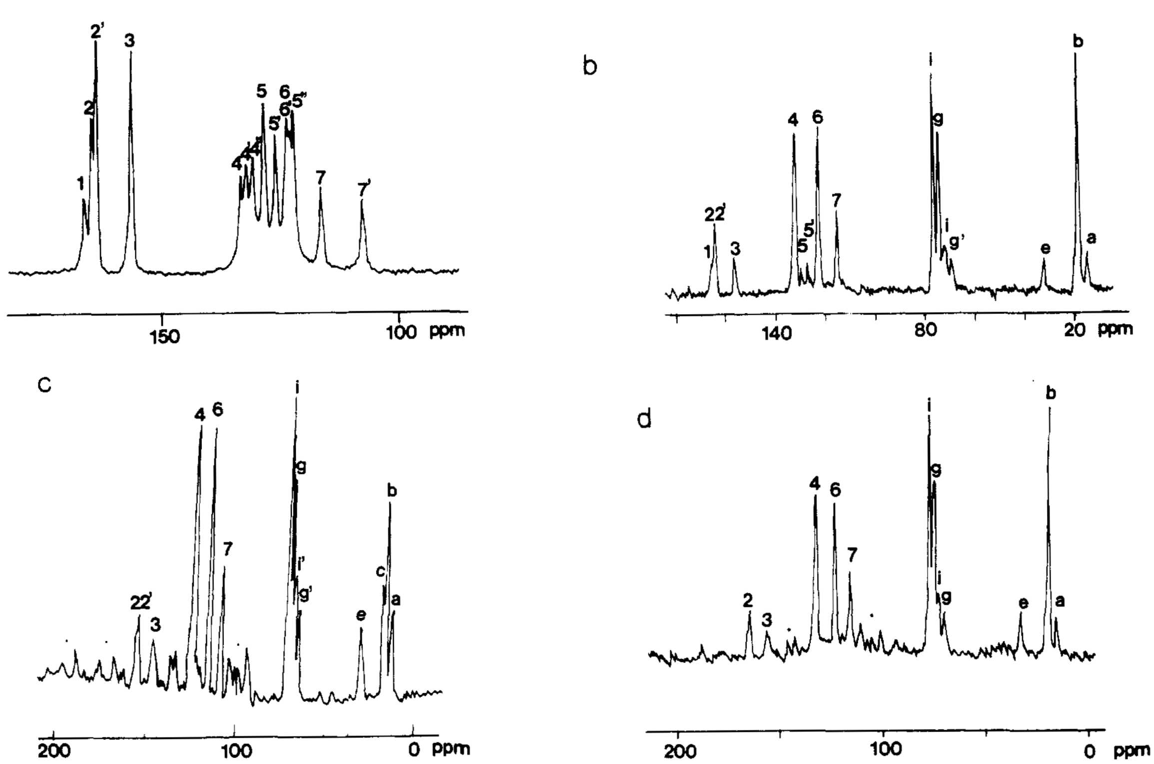

Figure 3. ^{13}C NMR spectrum of TLCM-III-PPG(725): (a) crystalline state at room temperature (CP); (b) smectic phase at 90 °C (DP); (c) isotropic state at 120 °C (DP); (d) isotropic state at 120 °C (CP).

and -PTHF(650). One would expect higher degrees of ordering in the smectic than in the nematic phase. It is unlikely that the increase of the size of S by about one monomer unit in the former macromolecule could result in greater freedom of rotation of the terminal butoxy groups in M. A probable explanation may be simply the temperature effect. In the case of TLCM-IIs, the NMR for the nematic state was studied at 40–45 °C, at which temperature the rotation of the C–O bond may be slow. On the other hand, the NMR of the smectic phase of TLCM-III-PPG(725) was recorded at 90 °C. These temperatures of investigation were dictated by the crystal to mesophase transition temperature (T_{KM}). The rotation of the C–O bond at 90 °C may be sufficiently rapid (>300 s^{-1}) so that the C7 and C7′, C4 and C″, and C6 and C6′ become equivalent. Furthermore, only two peaks were observed at 132.3 and 123.2 ppm, indicating that the aromatic ring is also undergoing rapid tumbling or torsional oscillation. The line width of a protonated aromatic carbon is about 70 Hz, which is about $1^1/_2$ times wider than in the crystalline state. All the aliphatic carbon peaks were resolved (see Table III). Also the line widths of aliphatic carbons decreased more than a factor of 2 (50 Hz) compared with the line widths in the crystalline state of 130 Hz. All these observations provide additional evidence that there is motional averaging of the dipolar interaction between ^{13}C and ^{1}H in the smectic state of TLCM-III-PPG.

The DP and CP spectra obtained at 120 °C for the isotropic state given in Figure 3c,d, respectively, are essentially the same. Furthermore, they differ from the spectrum of the smectic phase (Figure 3b) only in that the resonances of carbons b and c are resolved in the latter. The unexpected spectral similarities may be attributable to the fact that local microviscosity is high enough to render CP transfer[1] feasible. In other words, the TLCM has to be heated to above the coexistence temperature[9] to eliminate cross polarizations.

TLCM-III was also synthesized with PTHF(650) as the spacer. Its room temperature CP/MAS spectrum is shown in Figure 4a. The splitting of C7 and C7′ occurs at the same 116.6 and 108.5 ppm as in TLCM-III-PPG(725), but the C6 and C6′ and C4, C4′, and C4″ are not as well resolved. The line width for the aromatic carbons is about 65 Hz, which is about half that of the aliphatic carbons (130 Hz).

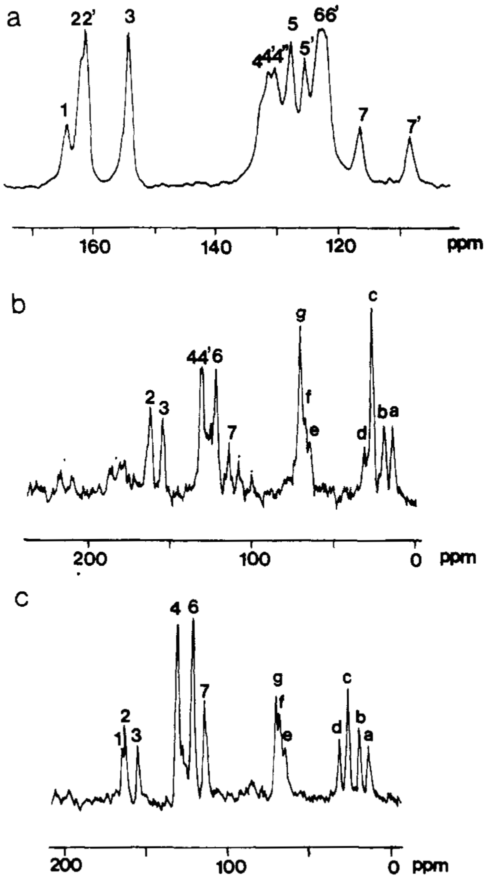

Figure 4. ^{13}C NMR spectra of TLCM-II-PTHF(650): (a) crystalline state at room temperature (CP); (b) mesophase at 80 °C (CP); (c) isotropic state at 110 °C (CP).

The CP/MAS spectra obtained at 80 °C (mesophase) and 110 °C (isotropic state) are shown in Figure 4b,c, respectively. Only isotropic chemical shifts were observed for the protonated aromatic carbons in both spectra. The splitting of carbon 7 disappeared at 20 °C below its T_{KM}. The aromatic lines became broader while the aliphatic ones were narrowed in the mesophase. These behaviors can be explained by the difference in motional rates at elevated temperatures (vide supra). Similar phenomena was also seen in poly(4,4′-bis(6-hydroxyhexoxy)biphenyl-2,4-toluenediisocyanate).[18]

The CP/MAS spectrum for TLCM-III-PTHF(2000) at room temperature is very different from all the above TLCMs below their melting temperatures. The aromatic region contains a featureless broad peak for the protonated carbons; only the nonprotonated carbons give resolved peaks. There is significant motional broadening of the mesogen. The line width of the methylene carbon is only 50 Hz, like in the mesophase. This indicates mobilty of the long spacer even in the crystalline state for this molecule.

Cross Polarization Transfer. The efficiency of magnetization transfer between ^{1}H and ^{13}C provides another measure of motion in addition to T_1 or $T_{1\rho}$. The technique involves irradiating the protons in the system at the Hartman–Hahn matching frequency.[19] During the time period in which the two spin systems are brought into contact, magnetization is transferred from the abundant protons to the "dilute" ^{13}C nuclei, thus significantly enhancing the carbon signal intensity. The efficiency of this process depends on the strength of the proton–carbon dipolar coupling, which to a first approximation in static systems depends on the proximity of protons to the ^{13}C nuclei. Carbons with directly attached protons will cross polarize more rapidly than nonprotonated carbons. However, the methyl carbons will have poor cross polarization efficiency because of the rapid methyl group rotation. The ^{13}C magnetization can be expressed[20] as a function of contact time, τ:

$$I = I_0\left[\frac{\exp(-\tau/T_{1\rho}{}^{H}) - \exp(-\tau/T_{CH})}{1/T_{CH} - 1/T_{1\rho}{}^{H}}\right] \qquad (3)$$

where $(T_{CH})^{-1}$ is the rate of cross polarization, and $T_{1\rho}{}^{H}$ is the proton spin–lattice relaxation time in the rotating frame. This equation predicts an initial increase in the magnetization intensity at short contact time at a rate given by $1/T_{CH}$, followed by decay of intensity for longer contact time determined by $T_{1\rho}{}^{H}$. Since cross polarization results only when there is static C–H interaction, carbon nuclei in different motional environments will cross polarize at different rates. A longer T_{CH} indicates more motion. Polarization transfer rates have been used by Laupretre at el.[21] to investigate the motional behaviors of poly(alkyl methacrylate) and thermotropic polyesters.

T_{CH} was obtained by fitting the observed profiles such as shown in Figures 5 and 6 to eq 3 with $T_{1\rho}{}^{H}$ fixed at the value calculated below for each case as given in Table IV. The resulting T_{CH} values are presented in Table V. In a rigid crystalline or glassy system T_{CH} is typically a few hundred microseconds, and the values for the crystalline phase of our TLCMs follow this expectation. The only exception is III–PTHF(2000) where the values are several times longer than expected. This cleanly indicates a greater segmental mobility in the longer chain PTHF system as compared to the shorter system.

Moving to the mesophase there are quite significant changes in the ability to cross polarize for the aliphatic parts of the molecule but not for the aromatic part. For the data of Table IV the aliphatic T_{CH} is at least twice that of the aromatic T_{CH} of the same molecule. The near conservation of the aromatic T_{CH} indicates that in the mesophase the aromatic moieties remain rigid whereas the aliphatic groups become mobile enough to significantly reduce the proton–carbon dipolar interaction.

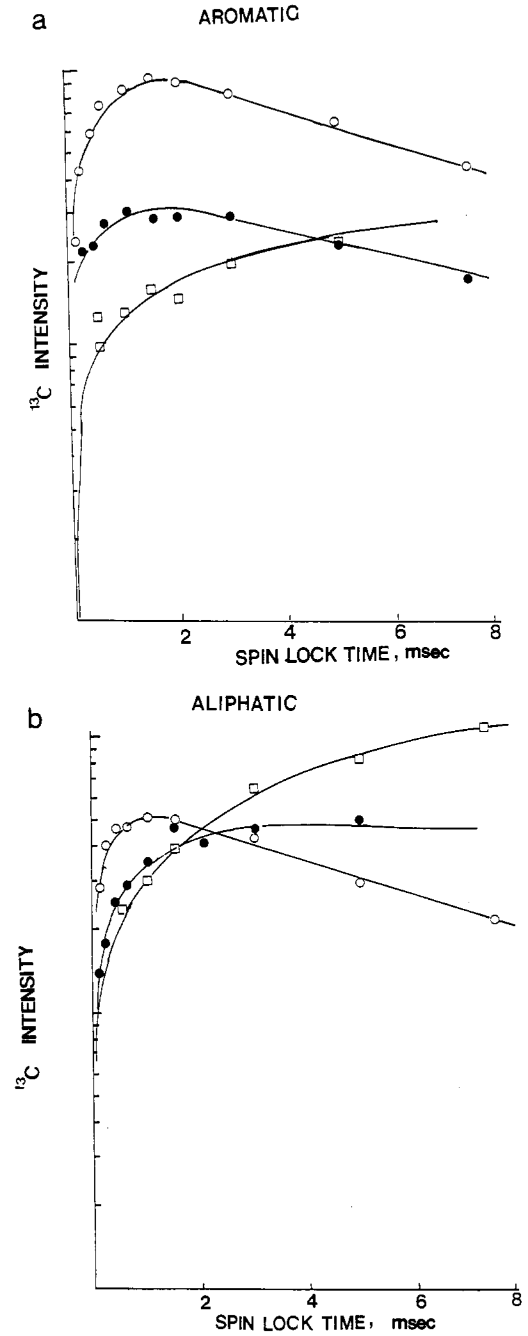

Figure 5. Variation of log intensity of (a) aromatic carbons and (b) aliphatic carbons versus contact time for TLCM-II-PTHF-(650) at three temperatures corresponding to the three states: (○) crystalline state at 0 °C; (●) mesophase at 40 °C; (□) isotropic state at 60 °C.

In the isotropic phase the T_{CH} values increase by about an order of magnitude due to the dramatically increased motion of the molecules as a whole. Interestingly some difference remains between the aromatic and aliphatic rates.

The logarithm of carbon intensity versus the spin-lock contact time for aromatic and aliphatic carbons in the TLCM-II-PTHF(650) system are shown in Figures 5 and 6. The other TLCMs yield similar plots. The proton spin-lattice relaxation time in the rotating frame, $T_{1\rho}{}^{H}$ was obtained from the slope of the decay of magnetization in

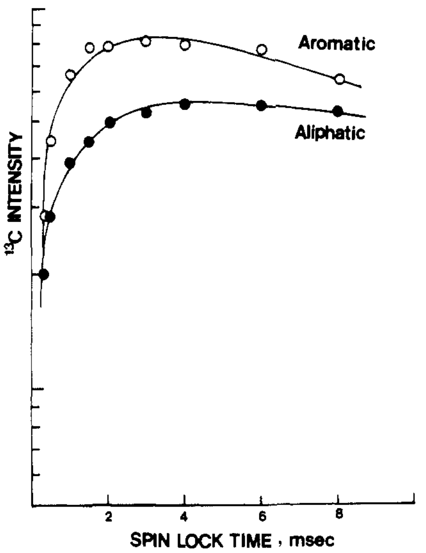

Figure 6. Variation of log carbon intensity versus contact time for TLCM-II-PPG(625) in the crystalline state.

Table IV
T_{CH} Values for TLCM

TLCM	carbon type	T_{CH}, ms crystalline	mesophase	isotropic
II-PTHF(650)	aromatic	0.13	0.18	2.3
	aliphatic	0.18	0.54	3.8
II-PPG(625)	aromatic	0.14		
	aliphatic	0.12		
III-PPG(725)	aromatic	0.16	0.19	1.2
	aliphatic	0.14	0.40	3.0
III-PTHF(650)	aromatic	0.21	0.30	
	aliphatic	0.16	0.57	
III-PTHF(2000)	aromatic	0.6		
	aliphatic	0.8		

Table V
$T_{1\rho}{}^{\mathrm{H}}$ Values for TLCM

TLCM	carbon type	$T_{1\rho}{}^{\mathrm{H}}$, ms crystalline	mesophase	isotropic
II-PTHF(650)	aromatic	7.3	16	N/A
	aliphatic	6.1	26	N/A
II-PPG(625)	aromatic	6.8		
	aliphatic	8.3		
III-PPG(725)	aromatic	7.5	32	62
	aliphatic	8.2	34	470
III-PTHF(650)	aromatic	11	14	
	aliphatic	11	29	
III-PTHF(2000)	aromatic	16		
	aliphatic	58		

such plots, and values are summarized in Tables IV and V.

In the crystalline state the values of $T_{1\rho}{}^{\mathrm{H}}$ for both the aromatic and aliphatic carbons are very close for each individual sample except TLCM-III-PTHF(2000). This indicates that the relaxations of the different types of protons either in the mesogen or in the spacer are averaged by spin diffusion.[22] This averaging will occur in the time $T_{1\rho}{}^{\mathrm{H}}$, approximately 10 ms in this case; if there are no domains larger than 20 Å or so, $T_{1\rho}{}^{\mathrm{H}}$ will appear the same for each species. In other words, the relaxation data show that there are no large separated phases of these two moieties except in the case of TLCM-III-PTHF(2000). In the mesophase relaxation data, the samples with PPG as the spacer give similar $T_{1\rho}{}^{\mathrm{H}}$ results in that the aromatic and aliphatic protons have the same, averaged values. However, in the mesophase for the PTHF spacer molecules, the averaging does not take place and distinct aromatic and aliphatic $T_{1\rho}{}^{\mathrm{H}}$ values are observed. Thus, in the mesophase there appears to be phase separation for the PTHF TLCMs but not for the PPG TLCMs. This observation is consistent with the rheological results.[8] The aggregation of the PTHF segments is probably due to the large difference in solubility parameter between the mesogen and PTHF when its chain length increases. $T_{1\rho}{}^{\mathrm{H}}$ increases with temperature for both moieties which implies that all the measurements are on the extreme narrowing side of the relaxation profile so that the segments are moving at a rate faster than 50 kHz.

In summary, line shape and cross polarization analyses yield discrimination of molecular mobility in the different stages of the liquid crystal transition. In particular the mobility of the aromatic and linear chain parts of the molecule are discriminated through cross polarization rates. In the PTHF spacer systems microphase separation is observed through the $T_{1\rho}{}^{\mathrm{H}}$ data.

Acknowledgment. This work was supported by a grant from the office of Naval Research and by the Materials Research Laboratory of the National Science Foundation at the University of Massachusetts, Amherst.

References and Notes

(1) Griffin, A. C.; Britt, T. R. *J. Am. Chem. Soc.* **1981**, *103*, 4957.
(2) Blumstein, R. B.; Stickles, E. M.; Blumstein, A. *Mol. Cryst. Liq. Cryst.* **1982**, *82*, 205.
(3) Jin, J. I.; Park, J. H. *Mol. Cryst. Liq. Cryst.* **1983**, *149*, 92.
(4) Buglione, J. A.; Roviello, A.; Sirigu, A. *Mol. Cryst. Liq. Cryst.* **1984**, *106*, 169.
(5) Emsley, J. W.; Luckhurst, G. R.; Shilstone, G. N.; Soga, I. *Mol. Cryst. Liq. Cryst.* **1984**, *102*, 223.
(6) Hoshio, H.; Jin, J. I.; Lenz, R. W. *J. Appl. Polym. Sci.* **1984**, *106*, 169.
(7) Chien, J. C. W.; Zhou, R.; Lillya, P. *Macromolecules* **1987**, *20*, 2340.
(8) Lin, Y. G.; Zhou, R.; Chien, J. C. W.; Winter, H. H. *Macromolecules* **1988**, *21*, 2014.
(9) Lin, Y. G.; Zhou, R.; Chien, J. C. W.; Winter, H. H. *Polymer* **1989**, *30*, 2204.
(10) Zhou, R.; Lin, Y. G.; Lillya, C. P.; Chien, J. C. W. *Macromolecules*, to be submitted for publication.
(11) Scheafer, J. In *Topics in Carbon-^{13}NMR Spectroscopy*; Levy, G. C., Ed., Wiley: New York, 1974; Vol. 1, p 149.
(12) Maricp, M. M.; Waugh, J. S. *J. Chem. Phys.* **1979**, *70*, 3300.
(13) Hays, G. R., *J. Chem. Soc., Perkin Trans. 2* **2 1983**, 1029.
(14) Uryu, T.; Kato, T. *Chem. Lett.* **1987**, 211.
(15) Uryu, T.; Kato, T. *Macromolecules* **1988**, *21*, 378.
(16) In the case of poly(*p*-hydroxybenzoate) (Fyfe, C. A.; Lyerla, J. R.; Valksen, W.; Yanroni, C. S. *Macromolecules* **1979**, *12*, 757), a 15° torsional oscillation of the aromatic C6 and C6′ carbons caused a 3.4 ppm difference in their chemical shifts. The similar behavior was reported for the linkage between the aromatic ring and the amide group in poly(*p*-phenyleneterephthalamide) (English, A. D. *J. Polym. Sci., Polym. Phys. Ed.* **1986**, *24*, 805). Even greater 180° flip of the aromatic ring was sensed in the crystalline state of poly(butyleneterephalate) (Jelinski, L. W.; Dumass, J. J.; Engel, A. K. *Macromolecules* **1983**, *16*, 403).
(17) VanderHart, D. L.; Earl, W. L.; Garroway, A. N. *J. Magn. Reson.* **1981**, *44*, 361.
(18) Smyth, G. Valle§pos, E. M.; Pollack, S. K.; Grebowiez, J.; Stenhouse, P. J.; Hsu, S. L.; MacKnight, W. J. *Macromolecules* **1990**, *23*, 2223.
(19) Hartman, S. R.; Hahn, E. L. *Phys. Rev.* **1952**, *128*, 2042.
(20) Andreis, M.; Koenig, J. L. *Adv. Polym. Sci.* **1989**, *89*, 132.
(21) Laupretre, F.; Jenkins, W. N.; Williams, G.; Noel, C. *Faraday Discuss. Chem. Soc.* **1985**, *79*, 191.
(22) The well-known proton spin diffusion process was discussed in our earlier works such as (a) Dickinson, L. C.; Yang, H. Y.; Chu, C. W.; Stein, R. S.; Chien, J. C. W. *Macromolecules* **1987**, *20*, 1757. (b) Parmer, J. F.; Dickinson, L. C.; Chien, J. C. W.; Porter, R. S. *Macromolecules* **1987**, *20*, 2308.

Registry No. II-PTHF (SRU), 110015-78-6; II-PPG (SRU), 110015-79-7; III-PTHF (SRU), 137122-86-2; III-PPG (SRU), 137122-87-3.